Impact of timing on trigger efficiency for LHCb Upgrade 2

Florian Harz[*]
CERN, EP-LBD

Abstract
I compared trigger efficiencies and rates for different LHCb trigger topologies for the upcoming detector upgrade 2 to evaluate the impact of using timing information in the trigger algorithms versus not using time information from the VELO subdetector. Not all trigger topologies show a correlation in their performance with using time information over not using it. However, some trigger topologies show an advantage of using the time information over not using it. More detailed checks should be performed to validate or further improve the trigger algorithms and the usage of time information within them.

Keywords
CERN Summer student report; LHCb; Upgrade 2; Trigger; Timing.

1 Introduction

The VErtex LOcator (VELO) is the very first sub-detector of the LHCb detector. It is used to localize the primary vertices of the initial proton-proton collisions and reconstruct the tracks of the resulting decay products.

As of LHC Run 3, there are about 5 collisions per bunch crossing. The vertices and tracks in the VELO are identified and reconstructed purely based on three-dimensional spacial coordinates. However, LHCb Upgrade 2 is planned to take place in Run 5, the high-luminosity era of LHC. There, the expected number of collisions per bunch crossing will increase to about 40. The VELO will be confronted with a busy environment of many vertices and about 2000 tracks per event. To be able to successfully identify and reconstruct vertices and tracks, the VELO in Upgrade 2 will be extended to precisely measure the time in addition to the spacial location of its traversing particles.[1]

The addition of the time information of the vertices and tracks could be used in improving the trigger algorithms with respect to their efficiencies and rate reductions. I have analyzed the impact of utilizing time information based on trigger topologies from the current LHC Run 3 period.

This report is organized as follows: First, section 2 gives an overview of the current trigger topologies which are used in LHC run 3. Second, section 3 explains how the time information can be used in triggering, how the efficiencies of the triggers are measured as well as different aspects which were taken into account during this analysis. Third, section 4 shows the results on the study of the impact of using time in the different trigger topologies. Finally, section 5 concludes this report with a summary of the studies and an outlook to further probe the subject.

2 Trigger topology

In LHC Run 3, the LHCb detector has to cope with an average data rate of 30 MHz. For this purpose, a full software trigger is used to reduce the data rate in the first trigger stage to 1 MHz. A visualization of the trigger is shown in Fig. 1. In this work, we focus on the HLT1 trigger for the LHCb upgrade 2 which does a partial reconstruction of the full event.

[*]On leave from the Johannes Gutenberg-Universität Mainz in Germany.

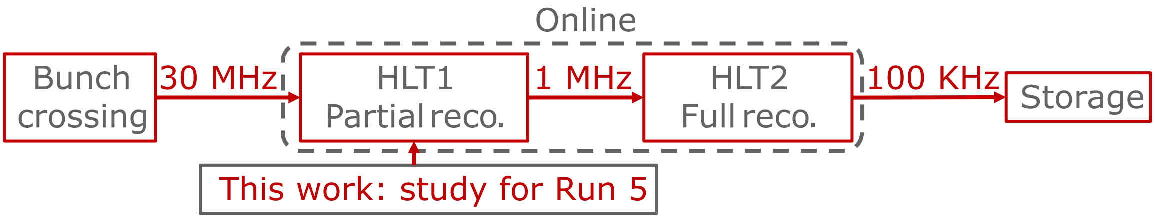

Figure 1: LHCb trigger configuration for LHC Run 3.

The trigger efficiency is measured for a simulated signal sample of $B_s \to D_s\pi$. The typical decay topology of the B_s-Meson is displayed in Fig. 2. Due to the long decay time of the B_s-Meson (the b-quark has to do a jump in flavor family in order to decay) and the large forward boost to hit the LHCb detector, the B_s-Meson has a measurable non-zero decay length resulting in a secondary vertex (SV) displaced from the initial primary vertex (PV) of the proton-proton collision. The tracks of the decay products from the B_s-Meson are displaced form the PV. This displacement can be quantified by calculating their impact parameter (IP) with respect to a PV. A large IP can be an indication for the track not to be created in the respective PV.

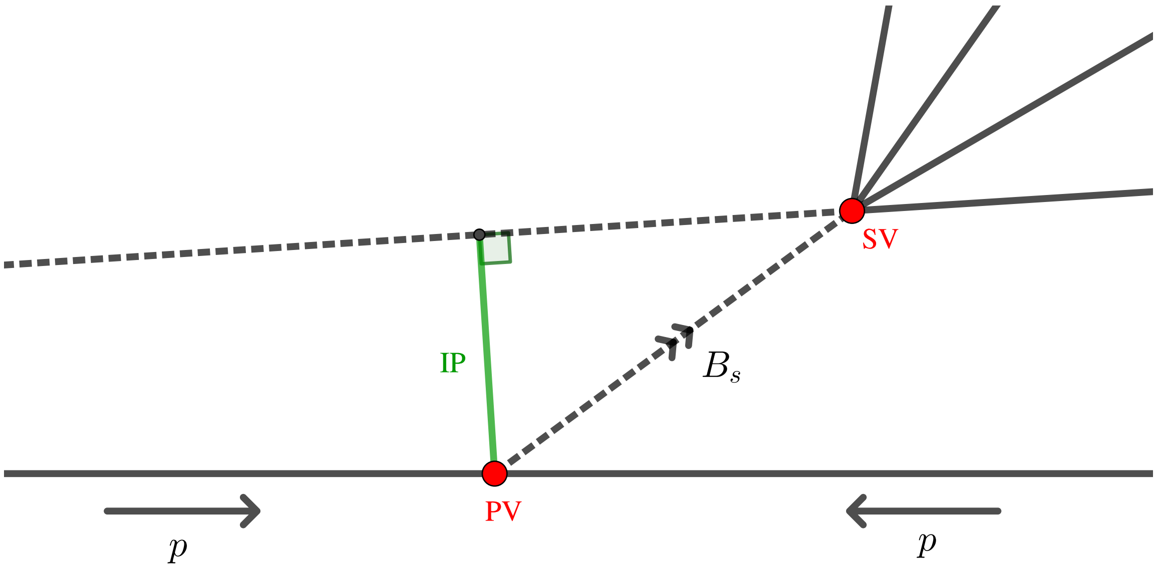

Figure 2: Typical decay topology of a boosted B_s-Meson. The depicted SV is supposed to be viewed as an effective vertex. In reality, one would also expect a non-zero flight distance of the D_s-Meson resulting in further secondary vertices.

Three different triggers have been explored in this work to trigger on the signal decay.

1. The 1-Track trigger looks at each track in an event individually and triggers the event capturing if at least one track looks promising.
2. The 2-Track trigger looks at each individual combination of two tracks in an event and tries to merge tracks that originate from the same SV. It triggers the event capturing if at least one track combination looks promising.
3. The 3-Track trigger looks at each individual combination of three tracks in an event and tries to merge tracks that originate from the same SV. It triggers the event capturing if at least one track combination looks promising.

3 Methodology

As stated before, the trigger efficiency is measured for a simulated signal sample of $B_s \to D_s\pi$. The trigger rate is measured with a minibias sample, which is supposed to represent the average proton-proton collision event. The number of events is shown in table 1. All events have been simulated for the proposed scenario A of the VELO in upgrade 2 (see [1] for more information). The vertices and tracks in these samples have been identified and reconstructed with timing information.

Table 1: Overview of the used MC samples.

Sample	N(Events)	VELO Scenario	Timing resolution [ps]
$B_s \to D_s\pi$	43286	S_A	50
Minibias	10100	S_A	50

3.1 Data structure

The simulated samples are a collection of events. Each event has (in case of the signal process) about 2000 reconstructed tracks and about 50 vertices. Each track and vertex is connected with their corresponding monte carlo (MC) track and vertex respectively, that contains the truth information of the object. In some cases, the reconstructed objects do not belong to any MC object. Each vertex has a 4D (x, y, z, t) position. Each reconstructed track has a first state with a 4D position, the slope of their track vector and their curvature in the detector to infer their momentum. The corresponding MC tracks have their full 4-momenta and particle ID.

3.2 Track time resolution

The simulation samples have been created for VELO scenario A which assumes a timing resolution of 50 ps. The technical design report (TDR) for VELO upgrade 2 predicts here a track time resolution of about 20 ps. I quantitatively verified this value (see Fig. 3) by calculating the time difference between the reconstructed tracks and the vertices of the truth matched MC particles. It is important to extrapolate both objects to the same location in space before comparing their time stamps. We can either use the 4-momentum of the MC particle to extrapolate its vertex location to the z-position of the reconstructed track or use the slope of the reconstructed tracks to extrapolate them to the z-position of the MC vertex. Both methods have been tested and no noticeable differences have been observed. This shows, that the mass of the particles can be neglected in the extrapolation of the tracks, as the track speed is assumed to be the speed of light.

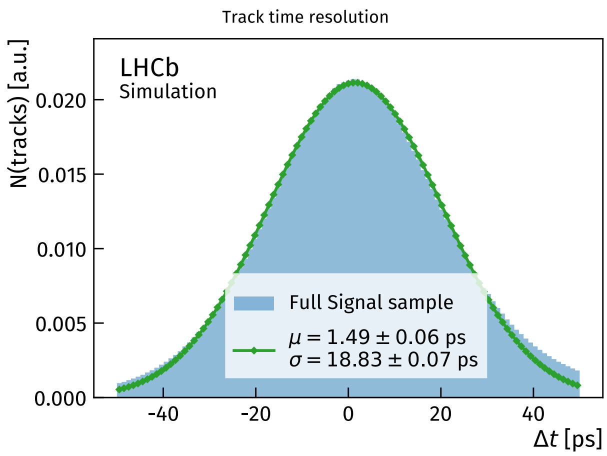

Figure 3: Resolution of the track time.

3.3 One-track trigger

The selection criteria used in the one-track trigger are listed in table 2 and are identical to the ones in the Run 3 one-track trigger defined in [2]. These cuts involve a preselection based on the transverse momentum of the tracks to filter out tracks with too low energies to be significant for coming from a B_s decay. Next, a combined cut based on the p_T and the χ^2_{IP} is imposed to filter out tracks that are not from secondary vertices. χ^2_{IP} is hereby used as a discriminator between tracks from primary vertices over tracks from secondary vertices where χ^2_{IP} tends to be larger for the later case. As we have multiple primary vertices in each event, we also calculate multiple χ^2_{IP} per track. Therefore, the primary vertex that yields the smallest χ^2_{IP} is used.

Table 2: Cuts used in the one-track trigger.

Variable	Cut
p_T	$p_T > 1\,\text{GeV}$
χ^2_{IP}, p_T	$\log(\chi^2_{IP}) > \begin{cases} \frac{1}{(p_T-1)^2} + \frac{1.2/25}{25-p_T} + \log(7.4) & , p_T < 25\,\text{GeV} \\ \log(7.4) & , p_T \geq 25\,\text{GeV} \end{cases}$

To further adjust the trigger a p_T re-tuning is used: $p_T \rightarrow p_T - \alpha$ where α is a freely adjustable parameter.

3.4 Two-track trigger

The selection criteria used in the two-track trigger are listed in table 3 and are identical to the ones in the Run 3 two-track trigger defined in [2]. First, some preselection based on p_T and χ^2_{IP} are applied to each single track. Next, pairs of two are chosen from the remaining tracks without permutations (we do not consider the combination $\{2, 1\}$ if we already considered combination $\{1, 2\}$). A fit-function is applied to each pair of tracks to calculate the best position of a secondary vertex where both tracks (could) originate from. Based on this SV and the tracks a new track is constructed that has passes through the SV with a momentum identical to the vector momentum sum of the tracks in the pair. This new track is supposed to describe the particle that decayed at the SV into the selected tracks (if these tracks originate from the same SV).

Table 3: Cuts used in the two-track trigger.

Object	Cut
Single tracks	$p_T > 500\,\text{MeV}$
	$\chi^2_{IP} > 6$
SV	$\chi^2_{SV} < 10$
	$p_T^{SV} > 2\,\text{GeV}$
	$2 < \eta < 5$
	$m_{\text{reconsructed}} > 1\,\text{GeV}$
MVA	$\alpha > \alpha_0$ with α_0 chosen to get 60 % background reduction.

On the SV and the SV track further selection criteria are applied. First, a cut on the goodness of the vertex fit, the χ^2_{SV}, is imposed. A fit on tracks that do not share a common SV is expected to yield a high χ^2_{SV}. Next, a cut on the transverse momentum of the SV, p_T^{SV}, is applied. Now, the best primary vertex, as an origin for the fitted SV track, is calculated by finding the primary vertex that minimizes the χ^2_{IP} for the SV track. The angle between the beam axis and the vector from the PV to the SV, represented by the pseudo rapidity η, is chosen to restrict the decay to the acceptance volume of the detector. In the end, a cut on the mass of the SV track is used to suppress decays from particles lighter than a B_s. However, a so called reconstructed mass $m_{\text{reconstructed}}$ is used which is defined as $m_{\text{reconstructed}} = \sqrt{m^2_{SV} + (p_{SV} \sin(\delta\theta))^2} + p_{SV} \sin(\delta\theta)$ with p_{SV} being the momentum of the SV track and $\delta\theta$ is the angle between the flight vector from the PV to the SV and the momentum vector of the SV track. The reconstructed mass is an estimation of the mass of the real particle from our signal process that decayed into three to four particles while only looking at two of these decay products.

To further suppress the track pairs, a deep neural network (DNN) to be used for multi-variate analysis (MVA) has been trained based on four variables from the secondary vertex and the SV track: The absolute momentum sum of the single tracks $\sum p_T = |p_T^{\text{1st track}}| + |p_T^{\text{2nd track}}|$, the χ^2_{SV}, the χ^2_{flight} as a measure of the displacement of the SV from the PV and the number of tracks with an χ^2_{IP} smaller than 16 (the number can be zero, one or two as we only look at pairs of two tracks). The DNN used is implemented with the Keras/Tensorflow library and consist of one normalization layer, followed by three hidden, dense layers and one softmax output layer with 2 output nodes (the value of the first node is a measure of how likely a given input is from a background process, the value of the second node is a measure of how likely a given input is from the signal process). The value of the second node is called score function α and is used to further reduce the amount of track combinations.

3.5 Three-track trigger

The three-track trigger is implemented on top of the two-track trigger. For every secondary vertex and SV track that is not filtered out by the two-track trigger a third track (which fulfills the same p_T and χ^2_{IP} cuts as the first two tracks from table 3) is added and a new secondary vertex based on the first secondary vertex track and the third track is fitted. A new SV track is calculated as well. As of now, no further cuts are applied on this three-track combination. Permutations between the first two tracks and the third track are allowed to always consider the case where two tracks come from a real secondary vertex (e.g. from the D_s) and the third track is displaced to them (e.g. the initial pion from the B_s decay). If we have the tracks 1, 2 and 3, we consider only their cyclic permutations: $\{(1, 2), 3\}$, $\{(2, 3), 1\}$ and $\{(3, 1), 2\}$ where the particles in the round brackets are the merged ones from the two-track trigger.

3.6 Trigger efficiencies and rates

The different triggers are applied on the signal sample and minibias sample. The number of events, where at least one track is selected, are counted. We separate three cases:

1. Trigger on signal (TOS): The event is selected if there is at least one track pair selected in which each track is considered as signal.
2. Trigger independent on signal (TIS): The event is selected if there is at least one track pair selected in which each track is not considered as signal.
3. Trigger on both (TOB): The event is selected if there is at least one track pair selected in which at least one track is considered as signal and at least one track is not consider as signal. This case does not exist in the one-track trigger as we need at least a pair of two tracks.

The trigger efficiency for the signal sample is defined as

$$\epsilon_{\text{sig}} = \frac{\text{N(TOS)}}{\text{N(all events)}}.$$

The minibias acceptance fraction is defined as

$$\epsilon_{\text{minibias}} = \frac{\text{N(selected events)}}{\text{N(all events)}}.$$

The acceptance fraction can be converted into a minibias rate via $R_{\text{minibias}} = \epsilon_{\text{minibias}} \cdot 30\,\text{MHz}$ with $30\,\text{MHz}$ being the average total event rate in LHC run 3.

3.7 Usage of time

There are different places in the trigger algorithms to use the time information of the tracks and vertices.

χ^2_{IP}

For the χ^2_{IP} we considered three different versions:

1. No time information is used in computing χ^2_{IP}. We call this a 3D χ^2_{IP}.
2. A $50\,\text{ps}$ time window is applied, selecting only primary vertices with a time difference smaller than $50\,\text{ps}$ with respect to the time of the track at the position of the vertex. For the vertices inside this time window a 3D χ^2_{IP} is calculated.
3. Instead of using a time window, the calculated time difference at a primary vertex is added directly to the value of χ^2_{IP}. We call this a 4D χ^2_{IP}.

The same χ^2_{IP} version used for the χ^2_{IP} cuts is also used to determine the best primary vertex.

Vertex fit

For the vertex fit function we considered two different versions:

1. No time information in determining the best production vertex of the given tracks is used.
2. Time information is used directly in the vertex fit function.

The χ^2 of the vertex fit is also calculated with the time information if it is used in the vertex fit itself. As the position of the secondary vertex can change by using a timeless version of the vertex fit every value that depends on the secondary vertex can be affected as well, e.g. the identification of the best primary vertex, the η between this PV and SV, the corrected mass and the χ^2_{flight}.

χ^2_{flight}

For the χ^2_{flight} we considered two different versions:

1. No time information is used. We have a 3D χ^2_{flight}.
2. Time difference is added directly in the 4D χ^2_{flight}.

4 Results

4.1 One-track trigger

The one-track trigger with a $50\,\text{ps}$ time window cut has been compared with the one-track trigger without this cut. Without any re-tuning, the one-track trigger gives the efficiencies and minibias rates listed in table 4. The efficiency with the time window cut increases by $2.81\,\%$ compared to the efficiency without time information. However, the minibias rate increases by $10.21\,\%$ at the same time.

Table 4: One-track trigger efficiencies and rates without p_T-re-tuning.

	Signal efficiency [in %]	Minibias acceptance fraction [in %]	Minibias rate [MHz]
With time window	75.83	88.15	26.44
Without time	73.76	79.97	23.99

The effect of the p_T-re-tuning is shown in Fig. 4. For a high minibias rate (which implies a small background reduction) the trigger with the time window performance as good as the trigger without the time information. However, for small minibias rates (which we have to achieve to stay within the available bandwidth limitations) the trigger with the time window cut gets outperformed by the trigger without the time window. Therefore, based on the current studies the usage of a time window for the one-track trigger can not be advised.

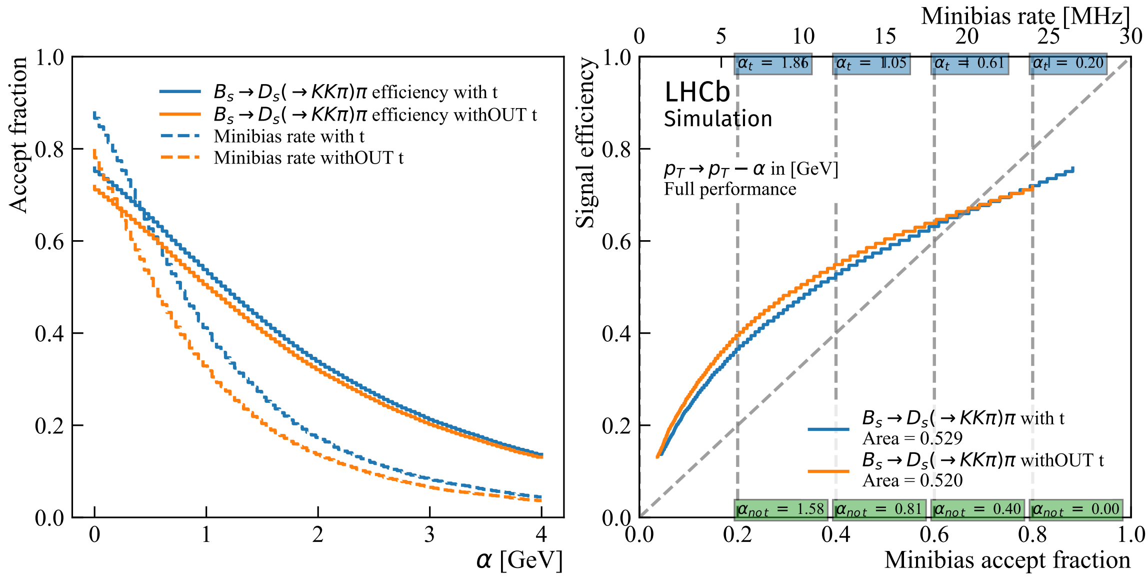

Figure 4: Effect of the p_T-re-tuning ($p_T \to p_T - \alpha$) on the signal efficiency and minibias rate for the one-track trigger while applying a 50 ps time window compared to not applying this time window. The left side shows the acceptance fraction of the signal and minibias for different values of α. The right side shows the same information by drawing the signal efficiency against the minibias rate for different values of α. The curves do not start with the total rate because the preselection (for $\alpha = 0$ GeV) is included.

4.2 Two-track trigger

For the two-track trigger with time information the time has been used in the vertex fit, for calculating a 4D χ^2_{flight} as well as applying a 50 ps time window cut for the 3D χ^2_{IP}. It has been compared to the two-track trigger where no time information has been used and therefore also no time window selection has been applied. Without applying the MVA, the two-track trigger gives the efficiencies and minibias rates listed in table 5. The efficiency with the time information increases by $4.05\,\%$ compared to the efficiency without time information. The minibias rate decreases by $7.43\,\%$ at the same time. In contrast to the one-track trigger, the preselection in the two-track trigger shows a favor for the usage of time.

Table 5: Two-track trigger efficiencies and rates without applying the MVA.

	Signal efficiency [in %]	Minibias acceptance fraction [in %]	Minibias rate [MHz]
With time	63.24	77.27	23.18
Without time	60.78	83.47	25.04

Creating the MVA

All track combinations that pass all of the two-track trigger cuts (except the MVA cut) are saved and used as an input for training the DNN that is used in the MVA cut. The DNN is supposed to do binary classification deciding if the input comes from a signal decay or a background decay. Each stored TOS

SV and SV track is classified as signal. Each stored minibias SV and SV track is classified as background. However, tracks that originate from b-quark or c-quark decays are not used from the minibias. The DNN is trained on this set of signal and background samples. A fraction of the samples is not given to the DNN for training and is used for testing the DNN instead.

The behavior of the score function on the test samples is shown in Fig. 5. The clear separation between signal and background can be observed. The distribution of the signal score for the b- and c-quark decays from the minibias sample is approximately flat. This shows, that the DNN is not sensitive to these decays and does not influence them.

Applying the MVA

The impact of the DNN on the signal efficiency and minibias rate can be seen in Fig. 6. The left side of this figure shows, that the DNN behaves approximately the same if it is trained and applied on input with time information over input without time information. The right side of the figure shows, that including time information slightly improves the signal efficiency while keeping a constant minibias rate for high minibias rates. For small minibias rates, the two-track trigger with time information behaves identical to the version without time information. Therefore, the current studies can not draw a conclusion for using time information in the two-track trigger over not using time information. Further studies are needed.

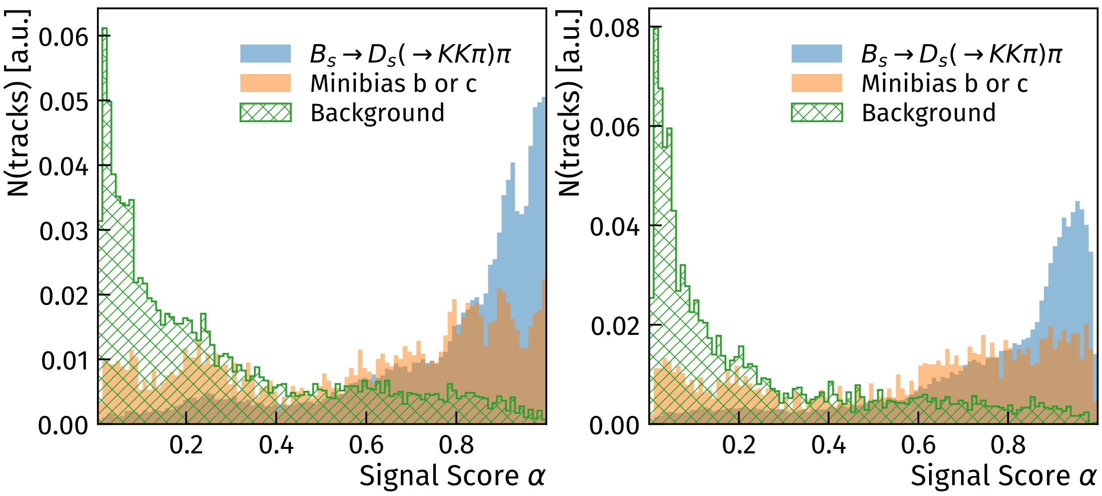

Figure 5: The distribution of the DNN score function for the signal and background test samples as well as the not trained on minibias samples where at least one track originates from a b- or c-quark. Left: Without using time information. Right: With using time information.

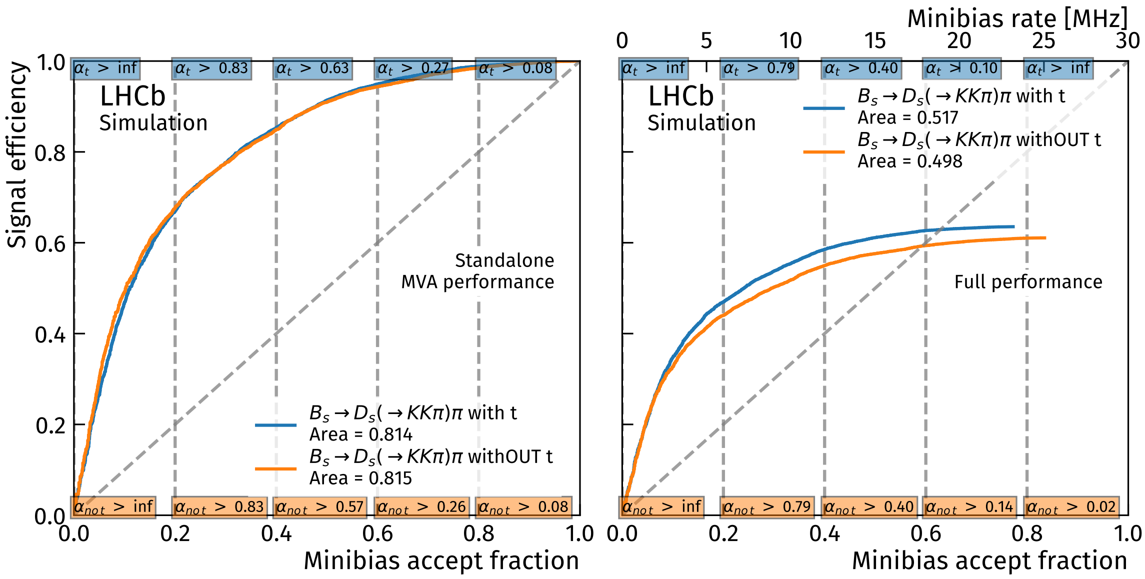

Figure 6: Effect of the DNN on the signal efficiency and minibias rate for the two-track trigger while using time information compared to not using time information. The left side shows the signal efficiency and minibias acceptance fraction for different cuts on the signal score from the MVA training. The right side shows the same information by including the preselection. Therefore, the curves do not start with the total rate.

4.3 Three-track trigger

As of now, only preliminary results exist for the three-track trigger. In the preselection with the two-track trigger, the MVA is applied by cutting on a fixed value of the score function of the DNN for which we expect to additionally decrease the minibias acceptance fraction to 40 %. No further cuts are applied yet and the three-track trigger gives the efficiencies and minibias rates listed in table 6. The rates in this table are smaller compared to table 5 from the two-track trigger case as it includes the MVA cut which previously has only been shown in Fig. 6. The efficiency with the time information increases by 3.89 % compared to the efficiency without time information. The minibias rate decreases by 24.93 % at the same time.

Table 6: Preliminary three-track trigger efficiencies and rates.

	Signal efficiency [in %]	Minibias acceptance fraction [in %]	Minibias rate [MHz]
With time	43.79	28.70	8.61
Without time	42.15	38.22	11.47

5 Summary and Outlook

The impact of using time information in the one-track, two-track and three-track trigger topologies on the signal efficiency and minibias rate has been studied for simulated data of the LHCb upgrade 2 in the HL-LHC Run 5 era.

For the one-track trigger no advantage of using the time information could be found over not using the time information. For the two track trigger a small increase in signal efficiency could be observed by using the time information while keeping the minibias rate constant. For the three-track trigger only preliminary results exists. However, a large decrease in minibias rate seems to be achievable by using time information while even slightly increasing the signal efficiency. Future studies should further analyze the three-track trigger by imposing cuts on the three-track combinations and creating a second MVA.

Further studies are needed on different signal modes and different detector scenarios to draw a final conclusion on how time information should be best made use of for LHCb upgrade 2.

Acknowledgments

I wish to thank Peilian Li and Sascha Stahl for being my awesome supervisors. I further would like to thank Dan Thompson, Tim Evans and Laurent Dufour for providing me with the simulation samples, the initial code base and helpful discussions. Finally, I would like to thank the whole LHCb group at CERN for welcoming me to their social activities and occasional gatherings during lunch and after work.

I wish to thank CERN and the summer student team for creating and maintaining the summer student program. I thank all summer students of this year for sharing their time with me and transforming this summer into an awesome and unique intercultural and international experience.

Bibliography

[1] C. (LHCb Collaboration. *Framework TDR for the LHCb Upgrade II - Opportunities in flavour physics, and beyond, in the HL-LHC era*. Tech. rep. Geneva: CERN, 2021. URL: https://cds.cern.ch/record/2776420.

[2] C. Fitzpatrick, J. M. Williams, S. Meloni, T. J. Boettcher, M. P. Whitehead, A. Dziurda and M. A. Vesterinen. *Upgrade trigger: Bandwidth strategy proposal*. Tech. rep. Geneva: CERN, 2017. URL: https://cds.cern.ch/record/2244313.